Title
Green's function for a planar phased sectoral array of dipoles: uniform high-frequency solution

ISBN
9780780356399

Authors
Capolino, F
Maci, S
Felsen, LB

Publication Date
1999

DOI
10.1109/aps.1999.789321

GREEN's FUNCTION FOR A PLANAR PHASED SECTORAL ARRAY OF DIPOLES: UNIFORM HIGH-FREQUENCY SOLUTION

F. Capolino[1], S. Maci[1] and L. B. Felsen[2]

[1]*Dept. of Information Engineering, University of Siena, Via Roma 56, 53100, Siena, Italy.*
[2]*Dept. of Aerospace and Mechanical Engineering and Dept. of Electrical and Computer Engineering, Boston University, 110 Cummington Street, Boston, MA 02215, USA.*

I. INTRODUCTION

In the first part of this paper [1], a truncated Floquet wave (TFW) formulation has been presented for the potential of a right-angle sectoral planar phased array of $\hat{u}$-directed dipoles (Fig. 1.1) (because repeated reference will be made to equations, figures, etc., in [1], all such references are preceded by 1.). In (1.11), we have shown a decomposition of the array potential $A(\vec{r})\hat{u}$ that can be more explicitly rearranged as follows,

$$A(\vec{r}) = \sum_{p,q} U_{pq}^{FW,1} U_{pq}^{FW,2} A_{pq}^{FW}(\vec{r}) + \sum_{q} U_{q}^{d,1} A_{q}^{d,1}(\vec{r}) + \sum_{p} U_{p}^{d,2} A_{p}^{d,2}(\vec{r}) + A^{v}(\vec{r}) \quad (1)$$

where $U_{pq}^{FW,i}$ $(i=1,2,)$ and $U_{q}^{d,1}$, defined in (1.7) and (1.12), are truncation functions that specify the shadow boundaries (Figs. 1.3, 1) pertaining to the domain of existence of the FW A_{pq}^{FW} (1.4) and of the edge-1 diffracted waves $A_{q}^{d,1}$ in (1.5) but with integration along the steepest descent path (SDP) passing through the pertinent SP. The vertex wave $A^{v}(\vec{r})$ is given by the integral in (1.1), but with local SDP integrations through the $(\bar{k}_{z1s}, \bar{k}_{z2s}) = (k\cos\beta_1,\ k\cos\beta_2)$ saddle point in both variables (Figs. 1.1 and 1.2). In this paper, we perform the asymptotic evaluation of the spectral wavenumber integrals, uniformly valid in the vicinity of the vertex and of the shadow boundary of any FW or edge-diffracted wave species (Fig. 1.3).

II. (TFW)-(EDGE DIFFRACTED WAVE) COMPENSATION MECHANISMS

The (TFW)-(edge-diffracted wave) compensation mechanism away from the vertex is formalized by the uniform asymptotic evaluation of $A_{q}^{d,1}$ in (1), which exhibits FW-modulated edge-diffracted waves with respect to the array edge along the z_1-axis. The uniform asymptotics is performed by the Van der Waerden (VdW) method as in [1.2], leading to

$$A_{q}^{d,1}(\vec{r}) \sim \frac{e^{-j\vec{k}_{q}^{d,1}\cdot\vec{r}}}{2d_1\sqrt{2\pi j\rho_1 k_{\rho 1,q}}} \left(B_2(k_{\rho 1,q}\cos\phi_1) + \sum_{p} \frac{[F(\delta_{1,pq}^2) - 1]}{jd_2 k_{\rho 1,q}(\cos\phi_{1,pq} - \cos\phi_1)} \right) \quad (2)$$

where $B_2(k_{z2})$ is defined in (1.2) and $(\rho_1,\ \phi_1)$ in Fig. 1.1; $\phi_{1,pq}^{SB} \equiv \phi_{1,pq} = \cos^{-1}(k_{z2,p}/k_{\rho 1,q})$ is the FW-shadow boundary (SB) angle (Fig. 1.3) with $k_{\rho 1,q} = (k^2 - k_{z1,q}^2)^{1/2}$ and $k_{z1,q}$ defined in (1.3). Furthermore, F denotes the transition function of the Uniform Theory of Diffraction (UTD) with argument $\delta_{1,pq} = (2k_{\rho 1,q}\rho_1)^{1/2}\sin[\frac{1}{2}(\phi_{1,pq} - \phi_1)]$. These conical diffracted waves, which are not affected by the z_2-domain p-indexed FW periodicity, provide the required continuity of the truncated FW fields across their shadow boundaries (Fig. 1.3.). The diffracted rays with wave vector $k_{q}^{d,1} = k_{z1,q}\hat{z}_1 + k_{\rho q,1}\cos\phi_1\hat{z}_2 + k_{\rho q,1}\sin\phi_1\hat{y}$ reach the observer along diffraction cones with angle $\beta_{1,q} = \cos^{-1}(k_{z1,q}/k)$, for $|k_{z1,q}| < k$ (see Fig.1) which are FW-modulated generalizations of the smooth-edge version in conventional GTD. Equation (2) is a simplified version of that presented in [1.2]; in (2), only the *propagating FW* (PFW) poles are regularized in the asymptotic process. This yields a more convenient, but still accurate, high-frequency algorithm. Note that $A_{p}^{d,2}(\vec{r})$ in (1) is obtained from (2) by interchanging 1 and 2 and q and p (see (1.3)).

0-7803-5639-X/99/$10.00 ©1999 IEEE.

III. UNIFORM VERTEX DIFFRACTION

Near the vertex, the z_1-edge and z_2-edge FW-shadow boundary transitions interact with the vertex-induced SBCs centered on the z_1-axis and z_2-axis, respectively, due to the truncation of the corresponding edge diffracted fields (Figs. 1, 1.3). The confluence of these four SB transitions near the vertex defines the asymptotics pertaining to vertex diffraction, which is obtained by the VdW method applied to the double integral $A''(\vec{r})$. Within the VdW method, the asymptotic evaluation of integrals characterized by specific arrangements of critical parameters (saddle points and singularities) is addressed by mapping the *given* integrand (both phase and amplitude) onto the simplest *canonical* integrand that accommodates the relevant configuration of critical points. The reduction to the canonical form is accomplished by selectively adding and subtracting "regularizing" portions of the integrand, which can involve an *arbitrary* number of poles; for simplicity here, we develop expressions only for regularization of the (p,q) pole which is closest to the saddle point (SP). For the vertex problem, the critical parameters are tied to the $(k_{z1},k_{z2})=(k_{z1s},k_{z2s})=(k\cos\beta_1, k\cos\beta_2)$ first order SP, and to the k_{z1}- and k_{z2}-poles in (1.3). We shall be satisfied here with the lowest order, locally uniform canonical asymptotics that extends over a limited region Q in the (k_{z1}, k_{z2}) spectral domain, large enough to accommodate the asymptotic isolation of the SP and poles at its boundary, and with its center defined by SP-pole coalescence. In Sec.III-A, we consider the proposed regularization architecture, and in Sec. III-B, we deal with the relevant asymptotics.

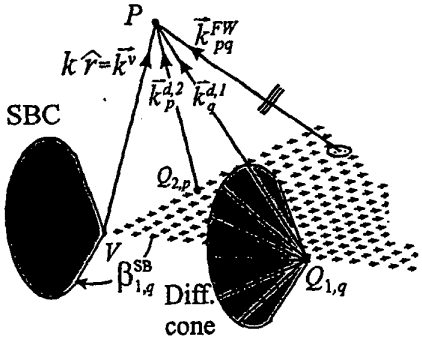

Fig. 1

A. Spectral regularization

The spectral regularizations of the integrand function $S(k_{z1},k_{z2})=B_1(k_{z1})B_2(k_{z2})$ in (1.1) are summarized in the Table, which we now explain. Starting in Table A with the spectral amplitude in the integrand of (1.1), we refer to the discussion in Sec.1.III on parameterizing the uniform sectoral array asymptotics in terms of the interaction, via the vertex, of the uniform semi-infinite array (SIA) solutions pertaining to each edge. These phenomenologies are identified in the first column, beginning sequentially with edge 1. The second column identifies the relevant spectral amplitude terms. Note that $B_{1,2}$ contains the pole singularities in the $k_{z1,2}$ integrations, respectively (see (1.2),(1.3)). The third column in Table A gives the VdW regularization which isolates, via the $W_{1,q}=[-jd_1(k_{z1}-k_{z1,q})]^{-1}$, $W_{2,p}=[-jd_2(k_{z2}-k_{z2,p})]^{-1}$ functions, the effect of the (p,q) poles under consideration. While the pole extraction is direct for edge 1, the corresponding treatment of edge 2 is more involved because it is preconditioned by the presence of edge 1. Altogether, the regularization of $S(k_{z1},k_{z2})$ leads to the nine individual terms in the *2nd* row of Table A, which are rearranged in the second column of Table B into four groups $S_i(k_{z1},k_{z2})$, $i=0,..,3$. Each group addresses uniform transition through a critical spatial domain listed in the first column. Note that these regularizing decompositions are *exact* for the propagating FW spectrum (evanescent effects are neglected here) and they provide the formal structure for subsequent uniform asymptotics. The lowest-order *locally* uniform asymptotic evaluation is performed next.

A: REGULARIZATION of the INTEGRAND in (1.1)

Constituent	*Coefficient*	*Regularization*
Edge-1 (1.5)	B_2 (1.2)	$B_2 - W_{2,p} + W_{2,p}$
Edge-2 effect on edge1	$B_1B_2 = \sum_{i=0}^{3} S_i$	$\begin{cases} B_2(B_1 - W_{1,q} + W_{1,q}) \\ -W_{2,p}(B_1 - W_{1,q} + W_{1,q}) \\ +W_{2,p}(B_1 - W_{1,q} + W_{1,q}) \end{cases}$

B: CANONICAL VERTEX REGULARISATION

Phenomenology	*Regularized coefficient*
near SB_1/SB_2 intersection	$S_0 = W_{1,q}W_{2,p}$
near SBC_1	$S_1 = W_{1,q}(B_2 - W_{2,p})$
near SBC_2	$S_2 = W_{2,p}(B_1 - W_{1,q})$
near vertex	$S_3 = S - S_0 - S_1 - S_2$

B. Asymptotic evaluation

The spectral decomposition in Table B leads to the exact spatial representation of the nonevanescent vertex diffracted field contribution,

$$A^v(\vec{r}) = A_0^v + A_1^v + A_2^v + A_3^v \tag{3}$$

where A_i^v $(i=0,\ldots 3)$ contains the spectral integrand $(8\pi^2 jk_y)^{-1} S_i(k_{x1}, k_{x2})\ e^{-j\vec{k}\cdot\vec{r}}$ of (1.1) and the (k_{x1}, k_{x2}) integration is performed near the real k_{x1}, k_{x2} axes along the local SDPs (Fig. 1.2). The asymptotics of A_i^v is dominated by the value of the integrands at the SP $(k_{x1}, k_{x2}) \equiv (k_{x1s}, k_{x2s}) \equiv (k\cos\beta_1, k\cos\beta_2)$, as determined from $(d/dk_{xi})(\vec{k}\cdot\vec{r})_s = 0$, $i=1,2$. Accordingly, $\vec{k}^v = \bar{k}_{x1s}\hat{x}_1 + \bar{k}_{x2s}\hat{x}_2 + (k^2 - \bar{k}_{x1s}^2 - \bar{k}_{x2s}^2)^{1/2}\hat{y} = k\hat{r}$ (Fig.1) and the SP phase is kr. Taylor expansion up to second order around the SP gives

$$\vec{k}\cdot\vec{r} \approx kr - \left(A(k_{x1} - \bar{k}_{x1s})^2 + 2H(k_{x1} - \bar{k}_{x1s})(k_{x2} - \bar{k}_{x2s}) + B(k_{x2} - \bar{k}_{x2s})^2\right) \tag{4}$$

with $A = kr/(2k^2\sin^2\phi_2)$ $B = kr/(2k^2\sin^2\phi_1)$, $H = kr\cos\beta_2\cos\beta_1/(2k^2\sin^2\beta_2\sin^2\phi_2)$ (see Fig. 1.1). This quadratic form is the lowest order approximation to the exact phase over a limited region Q centered at the SP in the (k_{x1}, k_{x2}) domain, which is "sufficiently large" to uniformly accommodate the poles in the various spectral terms $S_i(k_{x1}, k_{x2})$ in Table B. Since the A_0^v integral is the only one that has two poles (one in each variable), its asymptotic evaluation is carried out first. The other integrals can be asymptotically evaluated by reduction of A_0^v. First, we change variables to $\xi = \sqrt{A}(k_{x1} - \bar{k}_{x1s})$, $\eta = \sqrt{B}(k_{x2} - \bar{k}_{x2s})$ to transform the quadratic phase in (4) into $\vec{k}\cdot\vec{r} \approx kr - (\xi^2 + 2w\xi\eta + \eta^2)$, with $w = H/(AB)^{1/2} = \cot\beta_1\cot\beta_2 = \cos\phi_1\cos\phi_2$.

Next, the regular slowly varying amplitude function $(k_y)^{-1}$ in the integrand (see Table B for S_0) is evaluated at the SP $(\xi,\eta) = (0,0)$ and removed from the integral, thereby isolating the canonical function

$$T(a_q, b_p, w) = \frac{a_q b_p}{j\pi\sqrt{1-w^2}} \int_{-\infty}^{\infty}\int_{-\infty}^{\infty} \frac{e^{j(\xi^2 + 2w\xi\eta + \eta^2)}}{(\xi - \frac{a_q}{\sqrt{1-w^2}})(\eta - \frac{b_p}{\sqrt{1-w^2}})}\, d\xi\, d\eta, \tag{5}$$

where $a_q = \sqrt{A(1-w^2)}\ (\bar{k}_{x1s} - k_{x1,q})$ and $b_p = \sqrt{B(1-w^2)}\ (\bar{k}_{x2s} - k_{x2,p})$. Note that the (ξ,η) integral in (5) is actually the *canonical* mapping, in the rigorous VdW method, from the original (k_{x1}, k_{x2}) integral onto the simplest spectral integrand that accommodates a 2-D first order SP and a simple pole in each variable. The normalization constant in (5) is such that $T(a,b,w)$ tends to unity for large values of the parameters a and b (*i.e.*, for poles far from the SP). The numerical evaluation of (5) can be performed as in [2] in terms of standard Generalized Fresnel Integrals. It should be noted that in the transition regime where the poles are close to the SP, a_q and b_p can be approximated up to second order by the simpler expressions

$$a_q \approx \sqrt{2kr}\ \sin\left(\frac{\beta_{1,q} - \beta_1}{2}\right), \qquad b_p \approx \sqrt{2kr}\ \sin\left(\frac{\beta_{2,p} - \beta_2}{2}\right) \tag{6}$$

The other terms A_1^v and A_2^v in (3), which possess poles in only one variable, can be

evaluated by using the ordinary transition function of the UTD as shown in (2). The final outcome is

$$A_i^v \sim S_i(\bar{k}_{z1s}, \bar{k}_{z2s}) \frac{e^{-jkr}}{4\pi r} \mathcal{T}_i , \qquad i=0,\dots 3 \tag{7}$$

where $\mathcal{T}_0=T(a_q, b_p, w)$, $\mathcal{T}_1=F(a_q^2)$, $\mathcal{T}_2=F(b_p^2)$, $\mathcal{T}_3=1$, with S_i identified in Table B. The vertex-diffracted wave (3)-(7) incorporates the transition from a vertex-dominated spherical wave to an edge-dominated cylindrical wave and it compensates for the discontinuities across the SBCs of edge diffracted rays along $\beta_{1,q}^{SB}=\beta_1$ and $\beta_{2,p}^{SB}=\beta_2$.

IV. NUMERICAL RESULTS

Numerical tests have been performed on a "large" square array of dipoles in order to validate the asymptotic solution in (7). The electric field has been derived from the potential by using a dyadic spectral form in the integrand of (1.1), which introduces a simple additional factor into (7). An element-by-element summation over the contribution from each dipole serves as a reference. The 10×10 element test array has equi-amplitude dipoles oriented along $\hat{u}=\hat{z}_1$ with interelement phasing $\gamma_1=\gamma_2=0$ and period $d_1=d_2=1.7\lambda$, $\lambda=2\pi/k$. In a spherical coordinate system (r,θ,ϕ) with origin at the center of the array and polar axis perpendicular to the array plane, the array radiates a broadside ($\theta=0^\circ$) main beam but, due to the large interelement distances d_1 and d_2, there are nine PFW_{pq}, with all combinations of $p=-1,0,1$ and $q=-1,0,1$. Also, there are three propagating diffracted waves $E_q^{d,1}$ with $q=-1,0,1$ arising from edge 1 since $|k_{z1,q}|<k$ for these q-indexes; all other diffracted waves from edge 1 are radially evanescent and can be neglected. The three edge-1 diffracted waves can compensate for the disappearence of all nine PFWs at the SB $\phi_{1,Pq}^{SB}$ in (1.7). The same applies to the diffracted field from every other edge. Each of the three edge-1 diffracted fields has a SBC at $\beta_{1,q}^{SB}$, $q=-1,0,1$, given by (1.12). The vertex-1 diffracted field compensates for the disappearence of all these edge diffracted waves at their SBCs, thereby providing continuity of the total radiated field. In the numerics, these compensations are based on refined VdW-*globally* regularized versions of the wavefields in Sec.III. The same mechanism applies to the diffracted field from each vertex of the square array. In Fig. 2, the E_θ and E_ϕ total electric field components are plotted vs. scan angle θ along a 45° arc at a distance $r=25\lambda$ from the center of the array, thus passing close to two vertexes (see inset in Fig.2) so as to enphasize the vertex effect. The three maxima are related to the $FW_{-1,-1}$, FW_{00},and FW_{11}. The dotted curves show the edge-truncated asymptotic FW and diffracted field solutions (1) without the vertex-diffracted field in (3). The solid curves show the complete asymptotic field in (1) with the *globally* regularized field in (3) as well as the reference solutions; both coincide on the scale of the drawing. The agreement between the complete asymptotic and the numerical reference solutions is quite satisfactory.

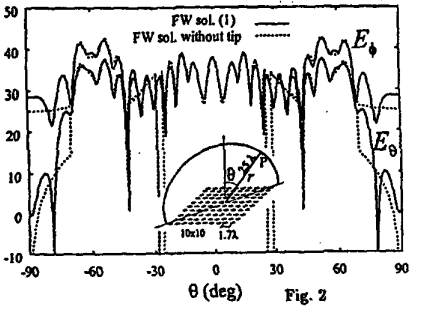

Fig. 2

REFERENCES

[1] F. Capolino, S. Maci, and L. B. Felsen "Green's function for a planar phased sectoral array of dipoles: synthesis via canonical constituents", *this symposium.*

[2] F. Capolino, S. Maci "Simplified, closed-form expressions for computing the generalized Fresnel integral and their application to vertex diffraction" *Microw. and Opt. Tech. Letters*, Vol. 9, N.1, pp. 32-37, May 1995.